Supporting Information

Rivas-Ubach et al. 10.1073/pnas.1116092109

SI Materials and Methods

Study Site and Experimental Design. The study was conducted in the Garraf Natural Park located in the Catalonian central coast (41°18′ N, 1°49′ E). The climate is Mediterranean with a pronounced 3-mo summer drought. The average annual rainfall is 550–600 mm. The maximum rainfall usually occurs in autumn (September–December). Average winter temperatures are around 7 °C, and the warmest summer temperatures average 22–24 °C.

Nine plots were established in March 1999. Six plots were subjected to a climate-change treatment: nighttime warming in three plots and drought in the other three. In the warming treatment, the nighttime temperature was increased by covering the vegetation with reflective covers that were retracted automatically when it rained, thus avoiding water exclusion. The drought treatment reduced rainfall input during spring and autumn (the rainy seasons in a Mediterranean climate). In this treatment the plot vegetation was covered automatically by a transparent plastic canopy during rain events; the canopy was removed when rain stopped. For details see refs. 1 and 2.

Sampling and Processing of Leaves. Sampling was conducted once per season from spring 2009 to winter 2010. Five individual plants in each plot were marked randomly as study subjects. A homogeneous fraction of the youngest leaves from each individual plant was frozen in situ in liquid nitrogen. Frozen leaves were lyophilized. Dried samples were ground with a Braun Mikrodismembrator-U (Biotech International) at 1,600 rpm for 8 min. All sample powders then were maintained at −20 °C until NMR extract preparation.

Leaf powder (200 mg) was introduced into a centrifuge tube. Six milliliters of 50% water–methanol mixture and 6 mL of chloroform were added to each tube (3). Samples were mixed for 15 s by vortex and then were sonicated for 1 min at room temperature. All tubes were centrifuged at 3,000 rpm for 30 min. Four milliliters of each fraction [aqueous (AF, polar phase) and organic (OF, nonpolar phase)] were collected independently into jars. This procedure was repeated twice to obtain 8 mL of AF and OF soluble fractions for each sample. OFs were collected by crystal syringes.

One hundred milliliters of water were added to AF samples to reduce the methanol percentage to approximately 5%. Samples were frozen at −80 °C and lyophilized. OF samples were placed separately in a round-bottomed evaporation flask and were dried in a rotary vacuum evaporator.

For the NMR analyses, 1 mL of KH_2PO_4-NaOD buffer in D_2O + 0.01% 3-(trimethylsilyl)propionic-2,2,3,3-d 4 acid sodium salt (TSP) was added to the dried AF samples to obtain a solution with final pH of 6.0. One milliliter of chloroform D plus 0.01% tetramethylsilyl (TMS) was added to dried OF samples. TSP and TMS were used as internal standards. All content was transferred to Eppendorf tubes and centrifuged for 3 min at 6,000 rpm and for 2 min at 10,000 rpm. For each sample, 0.6 mL of supernatant was transferred into NMR sample tubes.

NMR Experiments. NMR data acquisition for the metabolomic study was conducted through high-resolution ^{1}H NMR spectroscopy measurements. ^{1}H NMR spectra were acquired and processed based on described protocols with little modification (4–6). A Bruker Avance 600 spectrometer fitted with an automatic sample changer and a multinuclear triple resonance (TBI) probe (Bruker Biospin) and working at 14.1-T field strength (^{1}H frequency, 600.13 MHz) was used. The probe temperature was maintained at 298.0 K. Sample handling, automation, acquisition, and processing were controlled using TopSpin 2.1 software (Bruker Biospin).

Samples were allowed to equilibrate in the magnet for 1 min before the acquisition started. For the D_2O samples (polar phase), a conventional composite 90° ^{1}H pulse sequence with suppression of the residual water signal was used (7–9). The water resonance was presaturated using a power level of 55 dB during a relaxation delay (RD) of 2 s. Spectra were collected in the time domain as free induction decays (FIDs) across a spectral width of 9,615 Hz and during an acquisition time (AQS) of 1.7 s. A total of 128 transients were acquired in 32k data points. Each FID was zero-filled to 64k data points and multiplied by an exponential apodization function equivalent to a 0.2-Hz line broadening before Fourier transformation. The frequency-domain spectra were phase and baseline corrected automatically and were referenced manually to the TSP residual resonance at δ_H 0.00 ppm.

For the $CDCl_3$ samples (nonpolar phase), a standard 90° ^{1}H pulse sequence was used. A total of 128 transients were acquired in 32k data points across a spectral width of 9,591 Hz and during an AQS of 1.7 s and an RD of 2 s. As for the D_2O samples, FIDs were zero-filled to 64k data points, and an exponential apodization function equivalent to a 0.2-Hz line broadening was applied to the FID before Fourier transformation. Spectra then were phase and baseline corrected automatically and were referenced manually to the TMS residual resonance at δ_H 0.00 ppm. In all cases (D_2O and $CDCl_3$), when the automatic phase correction was not accurate, spectra were phase corrected manually.

Typical polar and nonpolar 1D ^{1}H NMR spectra profiles of *Erica multiflora* leaves are presented in Fig. 1 of the main text and in detail in Figs. S2 and S3 and in Table S4.

NMR Elucidation. For spectral resonance assignments, 1D and 2D NMR experiments were performed in selected samples of the water–methanol and chloroform extracts. A Bruker Avance 500 spectrometer (Bruker Biospin) equipped with a 5-mm high-sensitivity cryogenically cooled triple-resonance TCI probe with *Z*-gradients, operating at 11.7-T field strength (500.13 MHz ^{1}H and 125.76 MHz ^{13}C resonance frequencies), was used to perform the experiments. The probe temperature was maintained at 298.0 K. Sample acquisition and processing were controlled using TopSpin 1.3 software (Bruker Biospin).

1D ^{1}H NMR experiment and 2D ^{1}H-^{1}H correlation spectroscopy (COSY), ^{1}H-^{1}H total correlation spectroscopy (TOCSY), ^{1}H-^{13}C heteronuclear single-quantum correlation (HSQC), and ^{1}H-^{13}C heteronuclear multiple-bond correlation (HMBC) data were acquired using standard Bruker pulse sequences and routine conditions (6). For the water–methanol extract samples, 2D experiments were carried out with standard presaturation of the residual water peak. Spectra were referenced to TSP (^{1}H and ^{13}C at δ_H 0.00 ppm) in the D_2O samples and to the residual $CHCl_3$ (δ_H 7.260 ppm and 77.00 ppm for ^{1}H and ^{13}C, respectively) in the chloroform samples.

The concerted use of 2D ^{1}H-^{1}HCOSYand ^{1}H-^{13}C HSQC/HMBC experiments allowed the assignment of most of the peaks in the polar and nonpolar 1D ^{1}H NMR spectra profiles. When possible, assignments were confirmed with described data (11–34).

^{1}H NMR spectral resonance assignments, structural elucidated metabolites, and an example of a ^{1}H NMR spectrum with the main assigned peaks of the water–methanol extracts are shown in Table S4 and Fig. S3. The analog data for the chloroform extracts are collected in Table S4 and Fig. S2.

Chemical Analyses. ***C and N analyses.*** For each sample, 1.4 g of powder was weighed and introduced into a tin microcapsule.

C and N concentrations were determined by elemental analysis using combustion coupled to gas chromatography with a CHNS-O Elemental Analyzer (EuroVector).

P and K analyses. The P and K analyses were performed using acid digestion in a high-pressure, temperature-controlled microwave system. Briefly, 250 mg of leaf powder was weighed and placed in a Teflon tube, and 5 mL of nitric acid and 2 mL of H_2O_2 were added (10). A MARS Xpress microwave (CEM, Mattheus) was used to perform acid digestion. The temperature was increased to 130° over a 10-min ramp. Samples were maintained at this temperature for 5 min; then the temperature was increased to 200 °C over a 10-min ramp, and samples were maintained at 200 °C for 20 min. To finish digestion, the temperature was increased to 220 °C over a 5-min ramp and was maintained at 220 °C for 20 min.

All the digested contents were dissolved in 50 mL of water. After digestion, P and K were determined by optic emission spectrometry with inductively coupled plasma (Optima 2300RL ICP-OES; Perkin-Elmer).

Bucketing Procedure. To identify exactly where a peak begins and where it ends for all existing spectra peaks, a peak pattern for each sample type (polar and nonpolar) was created. Then the variable-size bucket table option of AMIX software (Bruker Biospin) was executed for the spectra to obtain all peak integral values scaled with respect to internal standards (bucketing).

1. Peñuelas J, Munné-Bosch S, Llusià J, Filella I (2004) Leaf reflectance and photo- and antioxidant protection in field-grown summer-stressed *Phillyrea angustifolia*. Optical signals of oxidative stress? *New Phytol* 162:115–124.
2. Beier C, et al. (2004) Novel approaches to study climate change effects on terrestrial ecosystems in the field: drought and passive nighttime warming. *Ecosystems (N Y)* 7: 583–597.
3. Lin CY, Wu H, Tjeerdema RS, Viant MR (2007) Evaluation of metabolite extraction strategies from tissue samples using NMR metabolomics. *Metabolomics* 3:55–67.
4. Beckonert O, et al. (2007) Metabolic profiling, metabolomic and metabonomic procedures for NMR spectroscopy of urine, plasma, serum and tissue extracts. *Nat Protoc* 2:2692–2703.
5. Kruger NJ, Troncoso-Ponce MA, Ratcliffe RG (2008) 1H NMR metabolite fingerprinting and metabolomic analysis of perchloric acid extracts from plant tissues. *Nat Protoc* 3: 1001–1012.
6. Kim HK, Choi YH, Verpoorte R (2010) NMR-based metabolomic analysis of plants. *Nat Protoc* 5:536–549.
7. Bax A (1985) A spatially selective composite 90-degrees radiofrequency pulse. *J Magn Reson* 65:142–145.
8. Gueron M, Plateau P, Decorps M (1991) Solvent signal suppression in NMR. *Prog Nucl Mag Res Sp* 23:135–209.
9. Zheng G, Price WS (2010) Solvent signal suppression in NMR. *Prog Nucl Magn Reson Spectrosc* 56:267–288.
10. Sardans J, Montes F, Penuelas J (2010) Determination of As, Cd, Cu, Hg and Pb in biological samples by modern electrothermal atomic absorption spectrometry. *Spectrochim Acta B* 65:97–112.
11. Fan TWM, Lane AN (2008) Structure-based profiling of metabolites and isotopomers by NMR. *Prog Nucl Mag Res Sp* 52:69–117.
12. Fan WMT (1996) Metabolite profiling by one- and two-dimensional NMR analysis of complex mixtures. *Prog Nucl Mag Res Sp* 28:161–219.
13. Walker TE, Han CH, Kollman VH, London RE, Matwiyoff NA (1982) 13C nuclear magnetic resonance studies of the biosynthesis by Microbacterium ammoniaphilum of L-glutamate selectively enriched with carbon-13. *J Biol Chem* 257:1189–1195.
14. Breitmaier E, Haas G, Voelter W (1979) *Atlas of Carbon-13 NMR Data,* Vol 1 (Heyden and Son, London) pp 1–215.
15. London RE (1988) C-13 labeling in studies of metabolic-regulation. *Prog Nucl Mag Res Sp* 20:337–383.
16. Iles RA, Hind AJ, Chalmers RA (1985) Use of proton nuclear magnetic resonance spectroscopy in detection and study of organic acidurias. *Clin Chem* 31:1795–1801.
17. Bolinger L, Seeholzer S, Kofron J, Leigh JS (1984) A guide to chemical shifts of 31-P, 1-H, and 13-C. *News Met Res* 1:32–45.
18. Brown JCC, Mills GA, Sadler PJ, Walker V (1989) 1H NMR studies of urine from premature and sick babies. *Magn Reson Med* 11:193–201.
19. Gromova M, Roby C (2010) Toward *Arabidopsis thaliana* hydrophilic metabolome: assessment of extraction methods and quantitative 1H NMR. *Physiol Plant* 140:111–127.
20. Duarte IF, Delgadillo I, Gil AM (2006) Study of natural mango juice spoilage and microbial contamination with *Penicillium expansum* by high resolution H-1 NMR spectroscopy. *Food Chem* 96:313–324.
21. Corse J, Lundin RE (1970) Diastereomers of quinic acid - chemical and nuclear magnetic resonance studies. Org Chem 35(6):1904–1909.
22. Dai H, Xiao C, Liu H, Tang H (2010) Combined NMR and LC-MS analysis reveals the metabonomic changes in *Salvia miltiorrhiza* Bunge induced by water depletion. *J Prot Res* 9:1460–1475.
23. Zhong XN, et al. (1998) Hydroquinone glycosides from leaves of *Myrsine seguinii*. *Phytochem* 49:2149–2153.
24. Govindaraju V, Young K, Maudsley AA (2000) Proton NMR chemical shifts and coupling constants for brain metabolites. *NMR Biomed* 13:129–153.
25. DeFrancesco JV, Witkowski MR, Ciolino LA (2006) GHB free acid: I. Solution formation studies and spectroscopic characterization by 1HNMR and FT-IR. *J Forensic Sci* 51: 321–329.
26. Nicholson JK, Timbrell JA, Sadler PJ (1985) Proton NMR spectra of urine as indicators of renal damage. Mercury-induced nephrotoxicity in rats. *Mol Pharmacol* 27: 644–651.
27. Ulrich EL, et al. (2007) BioMagResBank. *Nucleic Acids Res* 36(suppl 1):D402–D408.
28. Vlahov G (1999) Application of NMR to the study of olive oils. *Prog Nucl Mag Res Sp* 35:341–357.
29. Sacchi R, Addeo F, Paolillo L (1997) H-1 and C-13 NMR of virgin olive oil. An overview. *Magn Reson Chem* 35:S133–S145.
30. Jie M, Lam CC (1995) H-1-Nuclear Magnetic-Resonance Spectroscopic Studies of Saturated, Acetylenic and Ethylenic Triacylglycerols. *Chem Phys Lipids* 77:155–171.
31. Llusia J, Peñuelas J, Alessio GA, Estiarte M (2008) Contrasting species-specific, compound-specific, seasonal, and interannual responses of foliar isoprenoid emissions to experimental drought in a mediterranean shrubland. *Int J Plant Sci* 169:637–645.
32. Nemethy EK, Calvin M (1982) Terpenes from Pittosporaceae. *Phytochem* 21:2981–2982.
33. Gunstone FD (1995) *The Lipid Handbook* (Chapman and Hall, London) 2nd Ed.
34. The AOCS Lipid Library. Available at http://lipidlibrary.aocs.org/nmr/nmr.html. Accessed January 4, 2012.

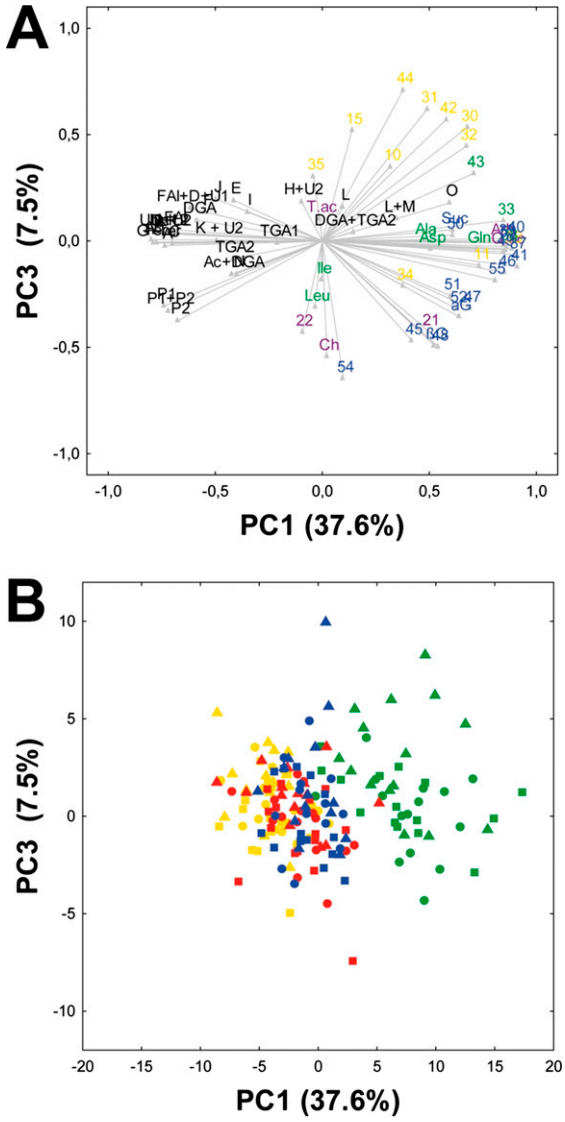

Fig. S1. Principal component analysis (PCA) plot from ^{1}H NMR metabolomic analyses of *E. multiflora* leaves using PC1 and PC3 axes. (*A*) Panel of metabolomic variables. Colors indicate different metabolic families: blue, sugars; green, amino acids; yellow; compounds related to amino acids and sugar plant metabolism; violet, secondary polar metabolites; black, nonpolar metabolites. Assignments are shown in Fig. 1 of the main text. (*B*) Panel of samples categorized by seasons. Colors indicate different seasons (red, summer; yellow, autumn; blue, winter; green, spring).

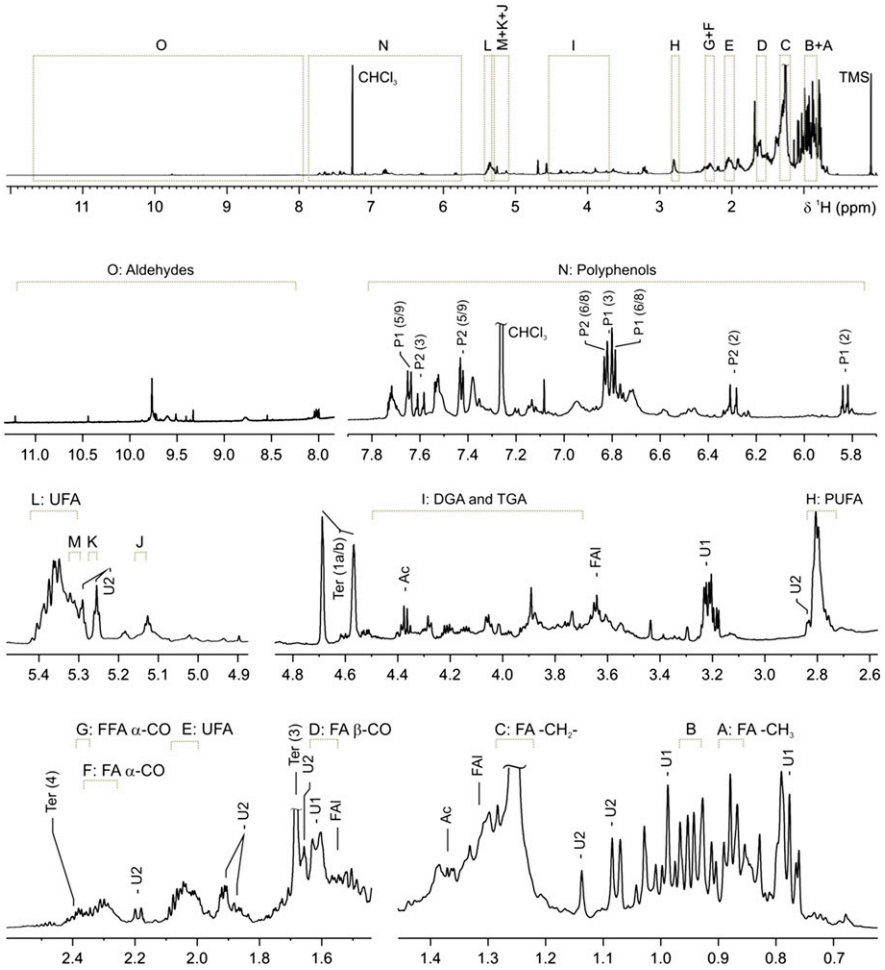

Fig. S2. Example of a 1D ^{1}H NMR spectrum of the chloroform extract sample of *E. multiflora* leaves. Assignments of the main peaks are indicated. The sample was dissolved in $CDCl_3$ and referenced to the residual solvent peak ($CHCl_3$). The spectrum was acquired at a 600-MHz magnetic field and at 298.0 K.

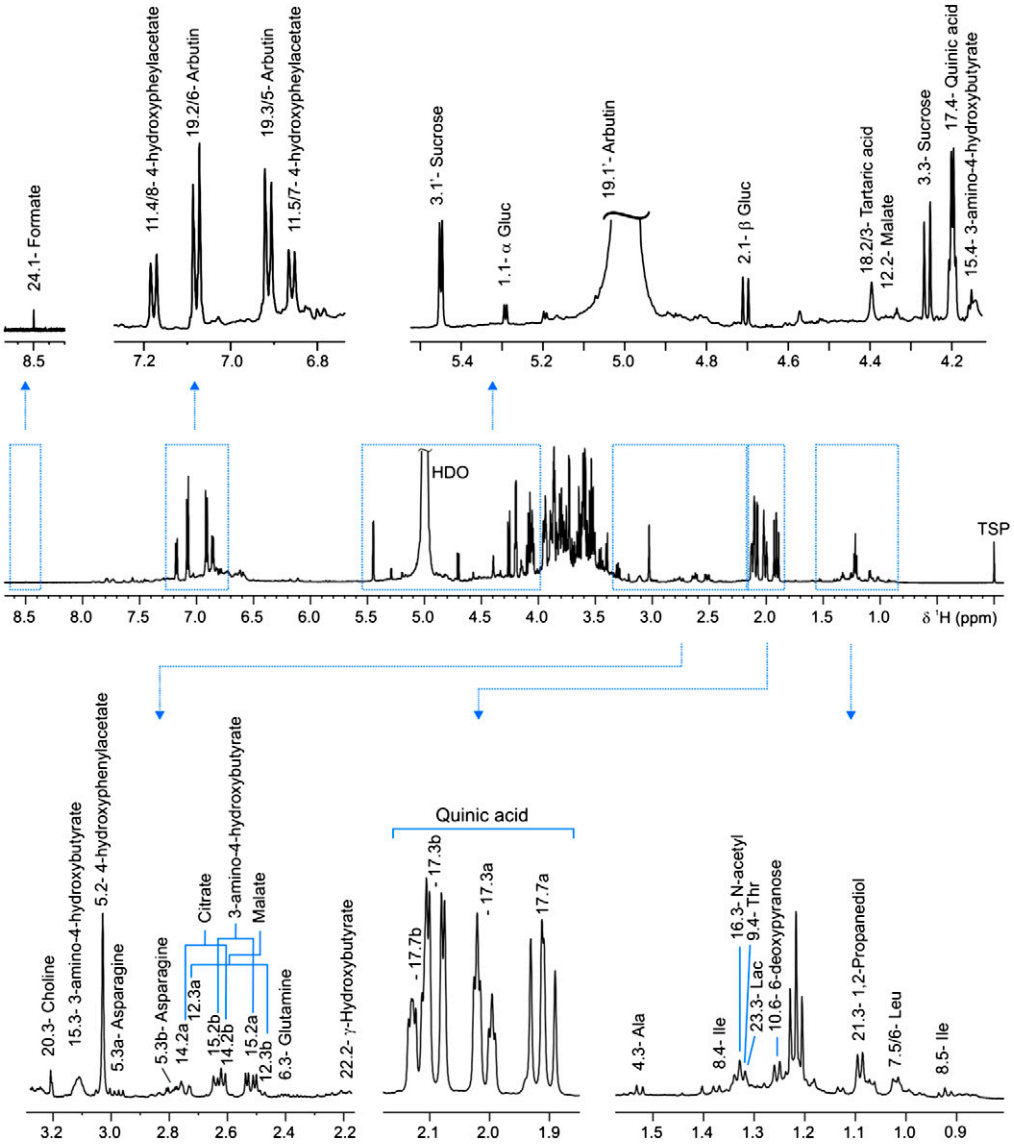

Fig. S3. Example of a 1D ^{1}H NMR spectrum of the H_2O/MeOH (1:1) extract of *E. multiflora* leaves with the assignment of the main peaks. The sample was dissolved in D_2O (pH 6.0) and referenced to TSP. The spectrum was acquired at a 600-MHz magnetic field and at 298.0 K.

Table S1. Foliar concentrations of metabolites and nutrients and nutrient stoichiometry in the different seasons and treatments

Table S1 (DOCX)

Data of metabolomic variables are the mean integral value with respect to TSP or TMS concentrations (0.01%). The statistical significances of season, treatment, and interaction were assessed with a mixed model for repeated measures of the stoichiometric and metabolomic variables. The MANOVA model included individual plants and plots as random factors and climatic treatment, season, nutrient stoichiometry, and metabolomic concentrations (under an unstructured correlation structure) and their interactions as fixed effects.

Table S2. Factors' statistical significance in the MANOVA and PERMANOVA conducted with the foliar concentrations of metabolites, nutrients, and the nutrient stoichiometries

Table S2 (DOCX)

The MANOVA model included individual plants and plots as random factors and climatic treatment, season, and stoichiometric and metabolomic concentrations (under an unstructured correlation structure) and their interactions as fixed effects. The PERMANOVA was performed using the Euclidean distance, with season (spring, summer, autumn, and winter) and treatments (control, drought, and warming) as fixed factors and block and individuals nested in block as random factors.

Table S3. Mean values of the score coordinates of the first four factors from the PCA conducted with the concentrations of metabolites and nutrients and the stoichiometric ratios (Fig. 2)

Table S3 (DOCX)

Last columns depict the results of one-way ANOVAs with respect to the year seasons (spring, summer, autumn, and winter). Different letters indicate significant statistical differences between seasons ($P < 0.05$, post hoc Bonferroni test).

Table S4. NMR assignments of the major metabolites in samples of H_2O/MeOH (1:1) and chloroform extracts

Table S4 (DOCX)

For samples dissolved in D_2O (pH 6.0), ^{1}H and ^{13}C NMR chemical shifts are referenced to TSP. For samples dissolved in $CDCl_3$, ^{1}H and ^{13}C NMR chemical shifts are referenced to the residual solvent peak.

Table S5. Foliar concentrations of all elucidated metabolites extracted from *Erica* spectra in the different climatic treatments (Control, Drought, Warming) within each season (Winter, Spring, Summer, Autumn)

Table S5 (DOCX)

Data are the mean integral value with respect to TSP or TMS concentrations (0.01%). Last columns depict the results of one-way ANOVAs.

Table S6. Mean values of the score coordinates of the first four factors from the PCA including metabolites and nutrient ratios presenting differences between climatic treatments (Fig. 3)

Table S6 (DOCX)

Last columns depict the results of one-way ANOVAs. Different letters indicate significant statistical differences between climatic treatments within each season ($P < 0.05$, post hoc LSD-Fisher test).